Materials Today Communications 38 (2024) 107995

Contents lists available at ScienceDirect

Materials Today Communications

journal homepage: www.elsevier.com/locate/mtcomm

Fractal analysis and microwave properties of La (Mg ½ Ti ½) O_3

Kouros Khamoushi [a,*], Cristina Serpa [b]

[a] Faculty of Engineering and Natural science, Tampere University, P. O. Box 1001, FI-33014, Tampere 33720, Finland
[b] Instituto Superior de Engenharia de Lisboa and Centro de Matemática, Aplicações Fundamentais e Investigação, Operacional, Portugal

ARTICLE INFO

Keywords:
Fractal analysis
Hausdorff dimension
Microwave materials
Dielectric ceramic materials
Electromagnetic properties

ABSTRACT

Fractal analysis was used to estimate the fractal dimensions and further define the structure of lanthanum magnesium titanium oxide. The microstructures and space groups of the materials were determined. This is relevant to the electrical properties at microwave frequencies, which are important for miniaturising electronic components. Fractal analysis or scanning mathematical algorithms of the microstructure were used for the first time in this study to determine the microstructure of the material, which demonstrates the novelty of this research. The shape, side, and angle calculations do not match those of the cubic structure. Based on the Bravais lattices in the cubic structure, the lattice parameters are equal, and all angles must be equal to 90°, whereas our results proved that the side parameters are not equal and at least one angle differs. The fractal regression analysis results showed that lanthanum magnesium titanate has a monoclinic structure with a $P2_1/n$ space group.

1. Introduction

A rare-earth material, lanthanum magnesium titanium oxide (LMT) [1,2], with a perovskite crystal structure, was examined in this study to measure its dielectric and electrical properties. This material can be used in electronic communications, such as intelligent transport systems, smart intelligent purposes, and the Internet of Things (IoT). Thus, this material can be used as a microwave filter in cellular phones. Microwave dielectric materials have been used for a wide range of applications as filter materials in telecommunications and wireless antennas. These materials have several applications: for example, in the miniaturisation of cell phones and in the communication of base station transmitters and receivers for high-quality telecommunications.

Another vital characteristic of microwave materials is their high-quality factor, which is the measurement of the energy loss or dissipation per cycle compared to the energy stored in the field inside the resonators. The loss tangent is inversely proportional to the quality factor, which is the result of the polarity variation based on the electromagnetic field.

Relative permittivity (ε_r) is inversely proportional to the dielectric wavelength. This is described by $\lambda_d = \lambda_0/\sqrt{\varepsilon_r}$, where λ_d the wavelength of the dielectric, and λ_0 is the wavelength in vacuum. The second factor is the temperature coefficient of the resonance frequency (τ_f). These materials must have τ_f as low as possible, near zero, to achieve exceptional relative permittivity (ε_r) [2,3]. The basic unit consists of corner-linked octahedra of X anions [4], with sites A and B typically located in the middle of the cube or at Site A. Octahedral ordering shifts the position of ions in the cube, which is a significant factor influencing the properties of the materials [5]. Ceramics have been used over the years because of their insulation properties and their application in alternating power lines to cores that endure cable wound resistors. Recently, ceramics have been used in various scientific fields, particularly in different fields of electronics [6] and electrical engineering. The crystal structure and space group of lanthanum magnesium oxide are currently being investigated.

Some researchers have suggested cubic structure for this material [7], whereas others believe that it is monoclinic or rhombohedral, and changes in the octahedral system have been reported [8]. The temperature and rotational movement of the octahedra affect the complete structure and cause it to bend in different directions. The A and B ordering of the cations in the corner and centre of the octahedra towards each other were bound together in the total structure. The tilting of the cation begins at different temperatures and, consequently, the material phase changes.

Fractal analysis was performed using the fractal regression method to examine the crystal structure of lanthanum magnesium titanium oxide and observe the atomic ordering of the material. This is a pioneering approach and recent methodology. The Hausdorff dimensions of the samples were measured by this technique. Characterisation was performed through mathematical identification of self-similarity. The

* Corresponding author.
E-mail addresses: kouros.khamoushi@tuni.fi (K. Khamoushi), mcserpa@fc.ul.pt (C. Serpa).

https://doi.org/10.1016/j.mtcomm.2023.107995
Received 2 November 2023; Received in revised form 12 December 2023; Accepted 27 December 2023
Available online 29 December 2023

fractal regression structure uses numerical computation analysis and a theoretical setting.

2. Experimental measurement

2.1. Electrical measurement

The electrical measurement of the quality factor (Q × f) and temperature coefficient of resonant frequency (τ_f) were performed at London South Bank University using a network analyser (Hewlett Packard-8719 C 50 MHz–13.5 GHz), and the τ_f of samples were measured at Filtronic, UK. The quality factor (Q × f) was tested using a cylindrical resonance cavity composed of high-conductivity metal with an interior approximately three times larger than the dimensions of the test sample. The test sample was placed inside the cavity with a low-loss, low-dielectric-constant support, and inductive coupling to the sample was achieved via a coupling loop or bent probe [10,11]. The transmission characteristics of the TE01δ resonant mode was measured, and the quality factor was calculated (Fig. 1).

The results of these tests confirmed that lanthanum magnesium titanium oxide with a temperature coefficient of resonant frequency of − 74 ppm/°C and a quality factor (Q × f) of 35000 at 8.1 GHz is a suitable material and can be an excellent dielectric material for microwaves and smartphones. An antenna in a normal network requires a frequency of 2 GHz with a phone frequency of approximately 800 MHz, and wavelength of approximately 18 cm. For smartphones, this is 9.375 cm. A normal 4 G mobile phone uses 700 MHz to 2.5 GHz frequency to transfer information between the origin and receiver in approximately 25 ms. The wavelength of such an antenna is approximately 10.71 cm and the normal length of a smartphone is between 15 and 20 cm.

2.2. Structure and characterization of microstructure

The X-ray outlines of the specimens are shown in Fig. 2; the entire sample exhibited a fitted crystal structure. The peaks from 1400 to 1675 °C agreed with the LMT structure.

Previously, a disordered 1:1 order cubic perovskite crystal structure was suggested for LMT [7], and later a monoclinic structure was suggested for the same material [9]. However, there are certain ambiguities in the definitions and space groups of the structure. In this study, we investigated this material to confirm its final structure.

In an earlier study, the structure of LMT has been reported as a cubic one (space group Pa3 a = 0.79 nm or a = 0.39 nm). Later [9], 1/2(111) superlattices and primary line splits were observed; however, no other structural information was provided [10–12]. Subsequently, the structure was refined and found to have a lower symmetry. However, there remains a contradiction in the assigned space groups.

Meden et al. [8] described a structure with a Pbnm space group,

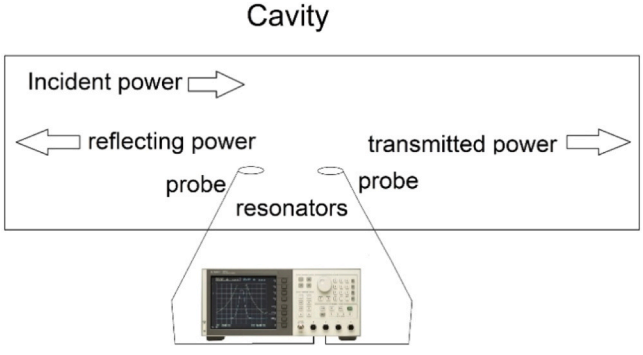

Fig. 1. Schematic device for measuring temperature coefficient factor and quality factor of samples.

whereas Lee et al. [9] used P21/n. Further lowering of the symmetry in $P2_1/n$ is not caused by the distortion of the unit cell but by the presence of only one B site in the Pbnm space group, and therefore, unable to describe the existing Mg/Ti ordering according to Glazer [4].

Superlattice reflections with specific combinations of odd (o) and even (e) Miller indices indicate the presence of definite peculiarities in the perovskite structure in-phase and anti-phase tilting of the octahedra, chemical ordering, and antiparallel shift of cations. By analysing the diffraction data, Lee et al. [9] suggested that LMT has an (a^- a^- c^+) tilting system. Extra peaks indicating phase tilting (eoo, oeo, and ooe) were not found in the X-ray diffraction pattern and could only be observed using high-resolution transmission electron microscopy (TEM). The X-ray diffraction (XRD) pattern of LMT powder is shown in Fig. 2. It was indexed based on the cubic perovskite unit cell Portable Document Format (PDF) card number 49–242. All the X-ray diffraction patterns of the calcined powders and sintered pellets were similar. Fig. 2 shows the appearance of the 1/2(111) peak. This was the result of the 1:1 chemical ordering of the B-site cations. The orthorhombic Pbnm space group has both in-phase and anti-phase tilting axes (a^- a^- c^+) or (a^- a^-a^-).For these reasons, the crystal structure of LMT must be described by the anti-phase tilting of the octahedra. Nevertheless, there is only one possibility to describe this structure: a material that has both in-phase and anti-phase tilting axes, (a^- a^- c^+) or (a^- a^- a^-), in addition to 1:1 chemical ordering. These results indicate that LMT has a monoclinic crystal structure with the space group $P2_1/n$ [13,14].

Based on this research, the monoclinic structure with space group $P2_1/n$ is closer to the LMT structure. The mathematical calculation of the microstructure and the analysis of Figs. 5 and 6 using fractal analysis of the LMT is testimony to this statement. Our recent investigation of the samples by XRD, SEM, and TEM did not clarify the microstructure properly, but a significant fractal analysis provided a clear image.

Fig. 2 shows the X-ray diffraction (XRD) traces of the LMT at various temperatures. The peaks were indexed according to portable document format (PDF) card number 49–242 and a pseudo-cubic perovskite unit cell with ≈ 0.39 nm. Siemens/Bruker D5000 X-ray Powder Diffraction (XRD) System was used to define the crystal structure of lanthanum magnesium titanate, based on the X-ray diffraction, SEM and TEM. Lattice parameters equal to a = 0.55 nm, b = 0.56 nm, and 0.78 nm and $\beta = 89.95°$ were attained, which shows the monoclinic shape, according to Glazer [4]. As shown in Fig. 2, X-ray diffraction patterns near 40° and 60° illustrate the (111) plane.

2.3. Scanning electron microscopy

Scanning electron microscopy of LMT is demonstrated in Fig. 3 [10], its sintering temperature was 1600 °C. This pellet was a single-phase dense ceramic with a grain size of 1–6 μm. Experimental materials with impurities show distinct phases that are not required. However, the prerequisite for this variety of materials is a homogeneous phase that does not exhibit distinctive contrast. The backscattering of our samples did not demonstrate any contradiction in the background colour. This was determined from the shape of the image that illustrated a standard and dense material, which is one of the conditions for single-phase ceramic materials. Scanning electron microscopy (SEM; JSM 6300, JEOL, Tokyo) was used to examine the phase evolution of the samples.

2.4. Structure of lanthanum magnesium titanium oxide

The X-ray diffraction pattern of the lanthanum magnesium titanium oxide powder is shown in Fig. 2. It was indexed according to lanthanum magnesium titanate PDF card number 49–242 with a single-phase cubic crystal structure. The XRD patterns of the samples did not show any expansion or cracking of the cubic peaks. All XRD patterns of the calcined samples were matched. High-resolution TEM (HRTEM) was performed to better define the crystal structure and space group of the

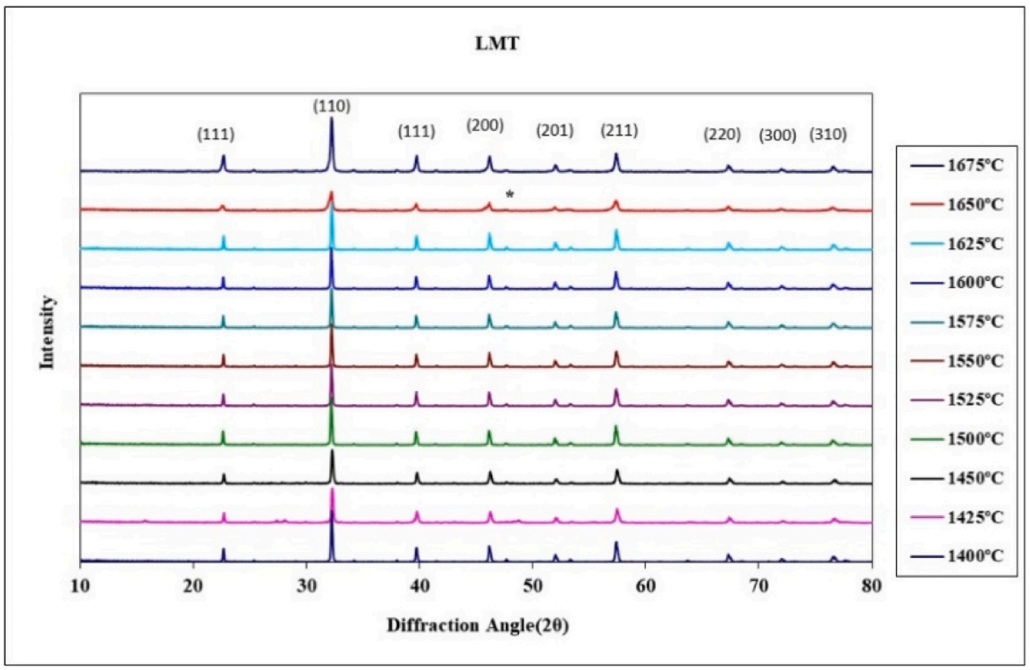

Fig. 2. X-ray diffraction patterns of LMT at 1400–1675 ℃.

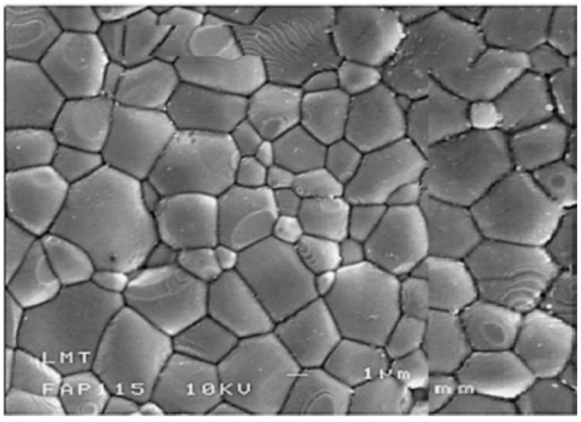

Fig. 3. Pellet of LMT at 1600 ℃ image illustrates dense single-phase material.

Fig. 4. Selected area diffraction pattern of LMT in the direction [111]. Ion milling model 600 GATAN Inc CA, device was employed for testing the structure of material. Transmission electron microscope (JEM, JOEL 2010, Japan) was used to identify the crystal structure of LMT.

samples.

We employed a transmission electron microscope (JEM 2010, JEOL, Tokyo) for phase evolution and used a selected area diffraction pattern (SADP) to index and examine the spot pattern of the sample. As shown in Fig. 4, the spot patterns indicate the atomic order of LMT with a regular structure. To obtain higher-quality samples, we used an Ion Milling Model 600 (GATAN Inc., California, USA). The device produces ultra-thin samples so that electrons can penetrate the TEM sample by shooting ions to the surface of it which is in the holder and can be rotated in different directions to be able to knock out ions from the surface of the specimen. The venting system of the Octogun device allowed the specimen chamber to operate at a low gas flow rate. The guns were in good thermal contact with the specimen chamber, operated at a high current, and did not require water cooling. Octoguns were typically operated using argon. These sample preparations were required to establish spot patterns.

2.5. Fractal analysis

This is the first mathematical fractal analysis method used to scan the grain boundaries and verify the structure of lanthanum magnesium titanate, demonstrating the novelty of this research. In practice, fractal methods and regression are used to study the structures, surface topographies, and dimensions of ceramic materials using a set of definite numbers. A fractal study of dimensions can be used for the development of surface morphology and multifractal parameters, making it conceivable to evaluate the regularity of the surface structure and the conditions of its construction. This method was used in this study to identify the grain boundaries by scanning the selected points initially and finally matching them with an estimated numerical set, which was measured using Fractal Real Finder software. This tool obtains a fractal function that approximates data. The plot of the results from the software illustrates the difference between the original and estimated values. In this

method, a portion of the grain boundary is selected from a sequence of points of this boundary as the input, and the data are organised by Cartesian or polar coordinates. The morphology of the surface produces an image in which it is feasible to compute the Hausdorff dimensions. Accordingly, we can observe the initial nature of the material and define its origin at the nanoscale level.

2.6. Mathematical setting

The mathematical analysis of irregular shapes is challenging for applied sciences. One approach is to consider the fractals. A fractal is a structure with special characteristics, namely, self-similarity and a refined shape at any scale, where the classical dimension is not adequate. We may find this type of structure in nature (e.g., clouds, vegetables, trees, flowers, and snails) and in several situations using real data. Classical fractal analysis uses estimates of fractal dimensions to characterise data. This type of measurement is used for fractal structures. A fractal dimension is a non-integer dimension that generalises a classical dimension. Some definitions are provided, such as Hausdorff and box dimensions. The Hausdorff dimension is a mathematical formulation with an abstract definition. In practice, box dimensions are typically estimated, which is an easy indicator to compute using computational algorithms.

The new method of fractal analysis proposed in the literature is more complete than the estimation of the fractal dimension. This is known as the fractal regression function method [16]. This is not only an estimation of the fractal dimension obtained but also the identification of the shape of the self-similarity property. This was performed using a fractal function that approximates the data. This characterisation enriches the analysis from the measurement to the shape. With a fractal function defined for certain real data, a larger analysis can be performed by analysing the theoretical characteristics of this mathematical function.

This method involves determining a fractal function that approximates data. The mathematical formulation of the fractal function used here was theoretically formulated and characterised in [17,18]. The modelled system is:

$$\varphi\left(\frac{x+j}{p}\right) = a_j\varphi(x) + b_j x + c_j,$$

where $x \in [0,1)$, $0 \le j \le p-1$, and a_j, b_j, c_j are the parameters (real numbers) to be estimated, with $0 < |a_j| < 1$. The default domain is [0,1). The solution of this system is the function $\varphi : [0,1) \to \mathbb{R}$ which is called a fractal function (refer [15]). It has been proven in [17] that such functions have mathematical fractal structures. The theoretical mathematical properties and explicit solutions are provided in [16–18].

The problem that is solved here (using the fractal regression method) is the estimation of the parameters a_j, b_j, and c_j that fit the real data. The first two are the fractal and directional coefficients respectively. The fractal characteristics are fundamentally determined by the a_j estimates. Fractal oscillations are strongly present when these values are larger in absolute terms. To define the system, p fractal periods and L fractal levels are required. Parameter p indicates the number of subintervals that the data are subdivided into, and the L refers to the number of times the self-similarity is analysed (replication process). Fractal Real Finder[1] software was used to perform numerical fitting. A few examples using this technique are provided in the literature, and we refer to the study of images of nanostructures collected onboard the International Space Station [20].

The Hausdorff dimensions can be estimated using an estimated fractal curve (refer [19]).

[1] For information and support material, see www.researchgate.net/profile/Cristina-Serpa.

Proposition. The Hausdorff dimension of the graph of the function φ solution of the above-mentioned system is upper bounded by the solution d of:

$$\sum_{j=0}^{p-1} \beta_j{}^d = 1,$$

where $\beta_j = \max\left\{\frac{1}{p}, |a_j|\right\}, 0 \le p \le p-1$..

Consequently, in practice, we estimate that the Hausdorff dimension is higher when the fractal coefficients a_j are higher. The fractal coefficient a_j is relevant if it is greater than $1/p$ (the inverse of the number of fractal periods). When all fractal coefficients were less than this value, the Hausdorff dimension of the data was estimated to be equal to the classical integer dimension.

2.7. Fractal reconstruction of images

The aim of this section is to identify the fractal structure shown in Fig. 3. We selected two parts and analysed them separately. For each, we selected a contour in which we marked red points equally spaced in a polar grid. We used two $p^L = 12^2 = 144$ angles, where a radius was assigned for each angle.

Using a numerical software, we obtained the coefficients a_j, b_j, c_j, for contours I and II (Tables 1 and 2). The corresponding graphical representations (points and estimated curves) are presented in Figs. 5 and 6.

The estimated fractal structure was characterised by fractal coefficients. If they are less than $\frac{1}{p} = \frac{1}{12} = 0.08(3)$, the fractal oscillations are not sufficiently large to influence the estimation of the Hausdorff dimension. In this context, we examine the relevant fractal coefficients to estimate this measure.

Only one relevant fractal coefficient exists for Contour I. This is $a_{10} = 0.087562$. The corresponding estimated Hausdorff dimension was 1.0017. For Contour II, the relevant fractal coefficients are:

$a_1 = -0.10634$, $a_6 = -0.143852$, $a_9 = -0.086732$, $a_{11} = -0.088802$ and its Hausdorff dimensions is 1.03713.

The above results indicated that Contour I was closer to a smooth curve than Contour II because the Hausdorff dimension was almost 1 (with only one relevant fractal coefficient) in the first case and was less than the estimate for the second contour, where the number of relevant fractal coefficients was larger.

Finally, both contours were reconstructed with a particularly good fit. The fractal self-similarity was successfully identified using a well-defined fractal function. The fractal nature of this material was analysed precisely and mathematically.

Fractal analysis and scanning mathematical algorithms were used for the first time in this study to determine the microstructure of the samples. The fractal images are illustrated in Figs. 5 and 6, and their calculated shapes, sides, and angles do not match those of the cubic structure.

According to the Bravais definition, in a cubic system, all parameters are equal, and the angles must be equal to 90°. From the fractal analysis and scanning mathematical calculations of the microstructure (Figs. 5 and 6), we observe that they are not.

Table 1
Contour I - Estimated coefficients for the fractal curve.

	0	1	2	3	4	5
a_j	0.066	0.012	-0.033	0.081	0.069	0.058
b_j	0.408	0.585	0.188	-0.074	-0.803	0.221
c_j	2.09	2.52	3.498	2.961	3.152	2.146
	6	7	8	9	10	11
a_j	0.048	-0.003	-0.013	-0.056	-0.088	-0.03
b_j	0.363	-0.076	1.354	0.006	-1.216	-0.785
c_j	2.478	2.876	3.028	4.562	4.634	3.142

Table 2
Contour II - Estimated coefficients for the fractal curve.

	0	1	2	3	4	5
a_j	-0.002	-0.106	-0.025	0.045	-0.053	-0.021
b_j	-0.396	0.849	0.218	-0.474	0.009	0.244
c_j	2.702	2.715	3.118	3.319	3.275	2.96
	6	7	8	9	10	11
a_j	0.144	-0.041	-0.038	-0.087	-0.018	0.089
b_j	-0.869	-0.234	0.861	0.539	-0.243	-0.583
c_j	3.239	2.692	2.606	3.348	3.499	3.096

Furthermore, all the sides had different lengths. In one corner of the structure, there are small differences between the results of original calculation (blue colour) and those estimated (yellow colour) by the software; this is due to the changes in β angle. A monoclinic crystal structure with space group $P2_{1/n}$ can be proposed for lanthanum magnesium titanate and neodymium zinc titanate, based on fractal analysis.

3. Conclusions

The fractal nature of the LMT was analysed using a new method called fractal regression with a good fitting approximation. We identified the fractal shape of this material in two different contours and concluded that the Hausdorff dimension was between 1.0017 and

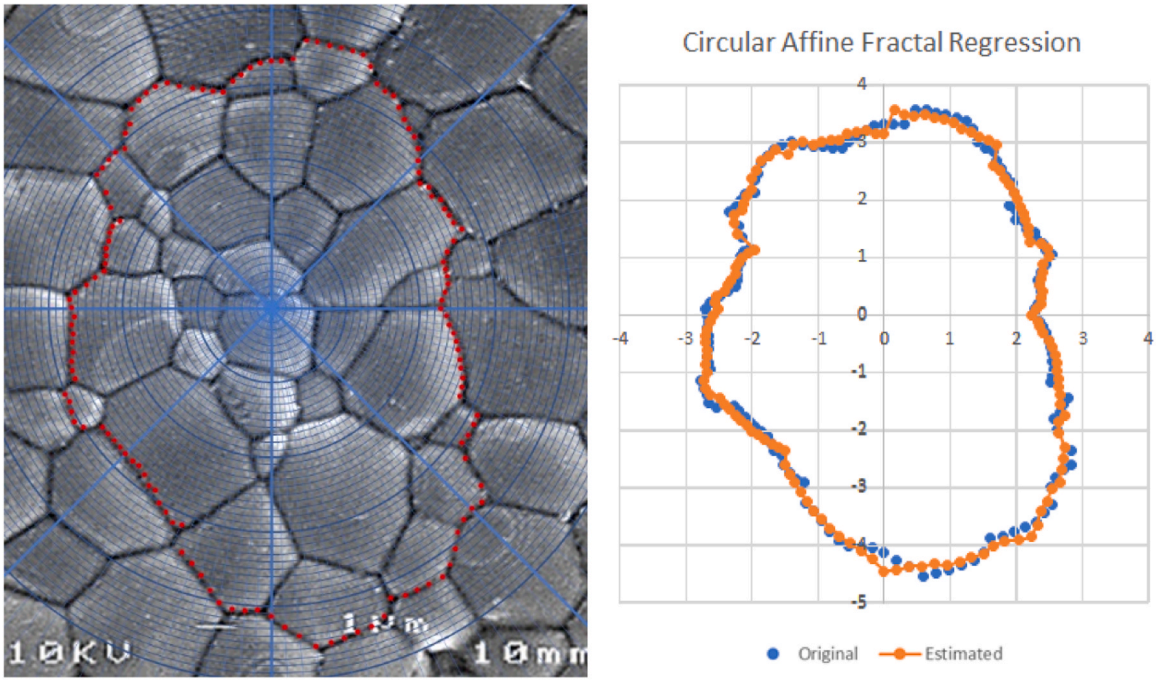

Fig. 5. Fractal analysis for Contour I.

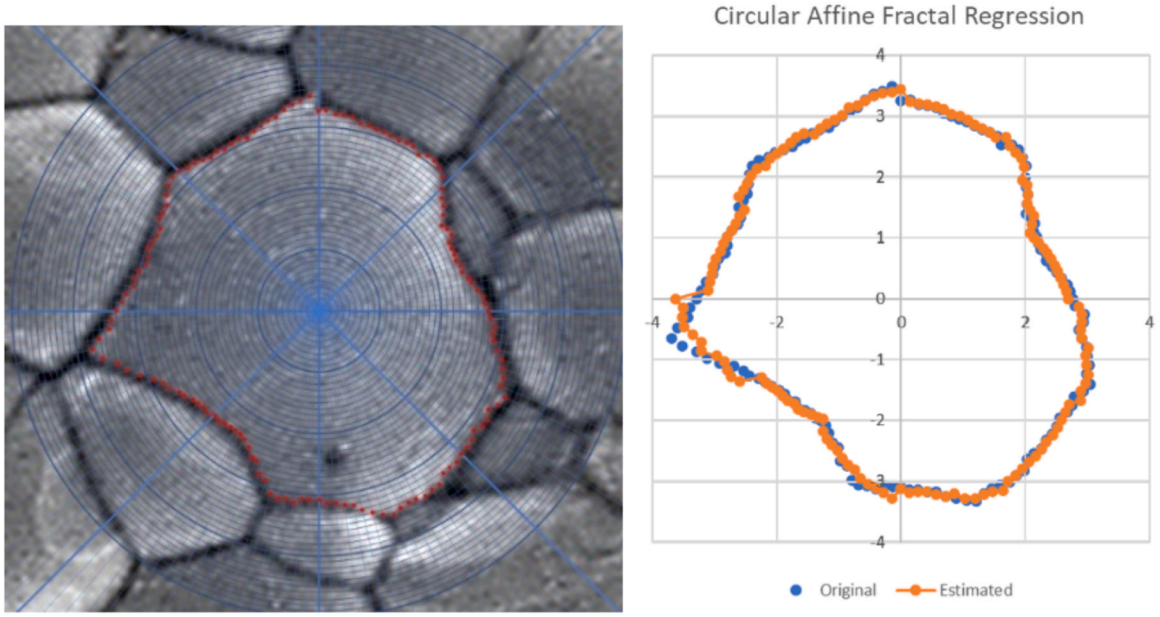

Fig. 6. Fractal analysis for Contour II.

1.03713. Some fractal characteristics were observed because this dimension is different from the Euclidean dimension. The crystal structure of the LMT samples was monoclinic, with a space group of $P2_1/n$ and a theoretical density of 6.08 g/cm^3. This material sintered from 1550 to 1675 ℃ to achieve a sintering density of approximately 99%. The temperature coefficient of the resonant frequency for the LMT was − 74 ppm/℃. The quality factor was 35000 at 8.1 GHz. This result proves that fractal analysis evaluates the fractal characteristics of the data. The fractal dimensions and additional fractal characteristics of a dataset determine how the grain boundary fits, enabling us to predict the properties of the materials. The significance of these findings is to improve these fractal dimension characteristics for further clarification and observation of microstructures. This analysis allowed us to further understand the intrinsic fine structure of the material, which was not visible to the human eye. Self-similarity is a concept that is present in nature and is worth examining it using mathematical tools and measuring accordingly. Fractal regression was the first instrument used in scientific literature to effectively reconstruct fractal self-similar functions from real data and to study this Issue. The fractal nature of the LMT was analysed using a new method called fractal regression with a good fitting approximation.

CRediT authorship contribution statement

Khamoushi Kouros: Writing – review & editing. **Serpa Cristina:** Software.

Declaration of Competing Interest

The authors declare that they have no known competing financial interests or personal relationships that could have appeared to influence the work reported in this paper.

Data Availability

Data will be made available on request.

Acknowledgments

Cristina Serpa acknowledges partial support from National Funding from FCT - Fundação para a Ciência e a Tecnologia, under the project: UIDB/04561/2020. Kouros Khamoushi expresses gratitude to Prof. Donald Lupo at Tampere University for his assistance.

References[1]

[1] K. Khamoushi, V. Mitic, G. Lazovic and S. Velikovic, 2019. Structure and dielectric properties of rare neodymium zinc titanate properties, Advanced Ceramics and Application VIII (Serbian Academy of Science, 2019). ⟨https://dais.sanu.ac.rs/123456789/6976⟩.
[2] G.S. Babu, V. Subramanian, V.R.K. Murthy, I-Nan-Lin, C. – T. Chia, H.-L. Liu, far infrared, Raman Spectroscopy, and microwave dielectric properties of La ($Mg_{0.5}$ Ti $_{(0.5-x)}$ Sn_x) O_3 Ceramics, page 1064906, J. Appl. Phys. Volume 102 (Issue 6) (2007), https://doi.org/10.1063/1.2778743. page 1064906.
[3] R. Ubic, Y. Hu, K. Khamoushi, I. Abrahams, structure, and properties of La (Zn½ Ti½) O_3, J. Eur. Ceram. Soc. Volume 26 (Issues 10-11) (2006) 1787–1790, https://doi.org/10.1016/j.jeurceramsoc.2005.09.033.
[4] Am Glazer, the classification of Tilted octahedra in Perovskite, Acta Crystallogr. 28 B (1972) 3384–3392, https://doi.org/10.1107/S0567740872007976.
[5] Hajime Ishikawa, Irene Munao, Bela E. Bode, Zenji Hiroia and Philip Lightfoot, $Na_2MoO_{2-\delta}F_{4+\delta}$ a perovskite with a unique combination of atomic orderings and octahedral tilts, Chem. Commun. (Issues 84) (2015), https://doi.org/10.1039/C5CC05446J.
[6] Y. Kim, K. Kim, D.Y. Son, et al., Printable organometallic perovskite enables large-area, low-dose X-ray imaging, Nature Volume 550 (Issue 7674) (2017) 87–91, https://doi.org/10.1038/nature24032.
[7] Girish Harshé, A.S. Bhalla, L.E. Cross, Synthesis and dielectric properties of a cubic perovskite: La ($Mg_{1/2}Ti_{1/2}$) O_3, Mater. Lett. Volume 18 (Issue. 4) (1994) 173–175, https://doi.org/10.1016/0167-577X(94)90225-9.
[8] A. Meden, M. Ceh, Structure determination and rietveld refinement of La (Mg½ Ti½)O_3, Mater. Sci. Forum Volume 278-281 (1998) 773–778, https://doi.org/10.4028/www.scientific.net/MSF.278-281.773.
[9] D.Y. Lee, S.J. Yoon, J.H. Yeo, S. Nahm, J.H. Paik, K.C. Whang, B.G. Ahn, Crystal structure and Microwave Dielectric properties of La (Mg½ Ti½) O_3 ceramics, J. Mater. Sci. Lett. Volume 19 (Issue 2) (2000) 131–134, https://doi.org/10.1023/A:1006603615193.
[10] K. Khamoushi, Processing and characterization of perovskite structure microwave dielectric ceramics. thesis for the degree of licentiate of technology, Tamp. Univ. Technol., Pages 124 (2009).
[11] K. Khamoushi, Cristina Serpa, Fractal Analysis and Ferroelectric Properties of Nd (Zn½ Ti½) O3 (NZT), Mod. Phys. Letter B 36 (36) (2023), https://doi.org/10.1142/s0217984922501676k.
[12] Eero Arola Kouros Khamoushi, Structure and dielectric properties of (La, Nd) (Mg½ Ti½) O_3, NORD-IS11, 22nd Nord. Insul. Symp. (2011) 1–4, https://doi.org/10.48550/arXiv.1502.0754.
[13] M.P. Seabra, V.M. Ferreira, Synthesis of La ($Mg_{1/2}$ $Ti_{1/2}$) O_3 ceramics for microwave applications, ISSN 0025-5408, Mater. Res. Bull. volume 37 (Issue 2) (2002) 255–262, https://doi.org/10.1016/S0025-5408(01)00748-6.
[14] M. Avdeev, M.P. Seabra, V.M. Ferreira, Structure evolution in La ($Mg_{1/2}Ti_{1/2}$) O_3–$SrTiO_3$ system, Mater. Res. Bull. volume. 37 (Issue 8) (2002) 1459–1468, https://doi.org/10.1016/S0025-5408(02)00809-7.
[15] Barnsley, F. Michael, Fractal functions and interpolation, Constrictive Approx. Volume 2 (1986) 303–329, https://doi.org/10.1007/BF01893434.
[16] Cristina Serpa, Affine Fractal Least Squares Regression Model, Fractals Volume 30 (Issue 07) (2022) 2250138, https://doi.org/10.1142/S0218348×22501389.
[17] Cristina Serpa, Jorge Buescu, Constructive solutions for systems of iterative functional equations, Constr. Approx. Volume 45 (2017) 273–299, https://doi.org/10.1007/s00365-016-9349-z.
[18] Cristina Serpa, Jorge Buescu, Explicitly defined fractal interpolation functions with variable parameters, Chaos, Solitons Fractals Volume 75 (2015) 76–83, https://doi.org/10.1016/j.chaos.2015.01.023.
[19] J. Buescu, C. Serpa, Fractal and Hausdorff dimensions for systems of iterative functional equations, J. Math. Anal. Appl. Volume 480 (Issue 2) (2019), https://doi.org/10.1016/j.jmaa.2019.123429. Pages 1-19.
[20] Vojislav Mitic, Cristina Serpa, Ivana Ilić, Markus Mohr, Hans-J.örg Fecht, Fractal nature of advanced Ni-based superalloys solidified on board the international space station, Remote Sens. Volume13 (Issue 9) (2021) 2021, https://doi.org/10.3390/rs13091724.